

A Precision-Scalable RISC-V DNN Processor with On-Device Learning Capability at the Extreme Edge

Longwei Huang, Chao Fang, Qiong Li, Jun Lin^(✉), Zhongfeng Wang^(✉)

School of Electronic Science and Engineering, Nanjing University, China

Email: {522022230032, fantasysee, qiongli}@smail.nju.edu.cn, {jlin, zfwang}@nju.edu.cn

Abstract—Extreme edge platforms, such as in-vehicle smart devices, require efficient deployment of quantized deep neural networks (DNNs) to enable intelligent applications with limited amounts of energy, memory, and computing resources. However, many edge devices struggle to boost inference throughput of various quantized DNNs due to the varying quantization levels, and these devices lack floating-point (FP) support for on-device learning, which prevents them from improving model accuracy while ensuring data privacy. To tackle the challenges above, we propose a precision-scalable RISC-V DNN processor with on-device learning capability. It facilitates diverse precision levels of fixed-point DNN inference, spanning from 2-bit to 16-bit, and enhances on-device learning through improved support with FP16 operations. Moreover, we employ multiple methods such as FP16 multiplier reuse and multi-precision integer multiplier reuse, along with balanced mapping of FPGA resources, to significantly improve hardware resource utilization. Experimental results on the Xilinx ZCU102 FPGA show that our processor significantly improves inference throughput by 1.6~14.6× and energy efficiency by 1.1~14.6× across various DNNs, compared to the prior art, XpulpNN. Additionally, our processor achieves a 16.5× higher FP throughput for on-device learning.

I. INTRODUCTION

Extreme edge platforms as Internet-of-things (IoT) nodes, such as in-vehicle and wearable smart devices, are confronted with significant challenges of constrained power supply, memory space, and computing resources, but there is a growing need to deploy computation-intensive tasks leveraging deep neural networks (DNNs) on these platforms. Hence, deploying quantized DNN models [1]–[5] emerge as an efficient solution at the extreme edge due to their substantial reductions on energy, storage, and computation costs.

Nevertheless, the efficient deployment of quantized DNNs on extreme edge platforms presents several challenges. Firstly, quantized DNNs [1]–[5] come in various precisions, ranging from 16-bit integers (INT16) to 2-bit integers (INT2), catering to different targeted applications. However, many processors [6]–[11] are unable to effectively perform precision-scalable operations, hindering the potential throughput improvement for these quantized DNNs. Secondly, extreme edge platforms require on-device learning capability [12] with floating-point (FP) precision to enhance model accuracy and preserve data privacy. However, existing precision-scalable processors [13]–[16] lack support for FP operations, making them incapable of realizing on-device learning. Finally, the resource requirements of extreme edge applications vary significantly, underscoring the importance of employing configurable hardware archi-

tures. In this case, FPGA devices [17]–[19] emerge as a promising alternative to CPUs and GPUs because of their superior energy efficiency, cost-effectiveness, and ability to be customized for specific applications. However, deploying BARVINN [15] and XpulpNN [20] on FPGA devices yields sub-optimal utilization of hardware resources, restricting the potential for achieving higher throughput in extremely edge quantized DNN applications. In summary, existing FPGA-based processors at the extreme edge requires three key improvements: supporting precision-scalable inference for various precision quantized DNNs, enabling floating-point computation for on-device learning, and increasing resource utilization on FPGA for higher throughput.

Therefore, in this paper, we propose a precision-scalable RISC-V DNN processor with on-device learning capability at the extreme edge using FPGA devices. Specifically, we design a re-configurable DNN processor that integrates a tightly-coupled co-processor into a PULP [21] cluster. The co-processor achieves a significant throughput improvement for DNNs by employing systolic computing dataflow on resource-efficient precision-scalable processing elements (PEs). The proposed PE supports various types of fixed-point inference for diverse quantized DNNs with precision ranging from INT16 to INT2, and enables FP16 operations that are widely used in on-device learning [22]. In addition, we leverage multiple techniques to improve hardware resource utilization including FP16 multiplier reuse, multi-precision multiplier reuse, and balanced mapping of FPGA resources. The main contributions of the paper are as follows:

- 1) Architecture of a high-throughput, energy-efficient and resource-efficient RISC-V DNN processor. By implementing a co-processor that leverages resource-efficient precision-scalable PEs with efficient systolic computing dataflow, our processor significantly improves both inference throughput and energy efficiency by up to 14.6× at various DNN precisions compared to XpulpNN [20].
- 2) Design of resource-efficient precision-scalable PEs. By integrating several hardware reuse techniques, we achieve a reduction of 25.8% and 7.9% in LUT and DSP overhead, respectively, for 8-bit precision-scalable multiplier trees. The saved resources can be used to add more PEs for further throughput improvement.
- 3) Method of boosted on-device learning throughput along with increased resource utilization. By reusing INT16

arXiv:2309.08186v1 [cs.AR] 15 Sep 2023

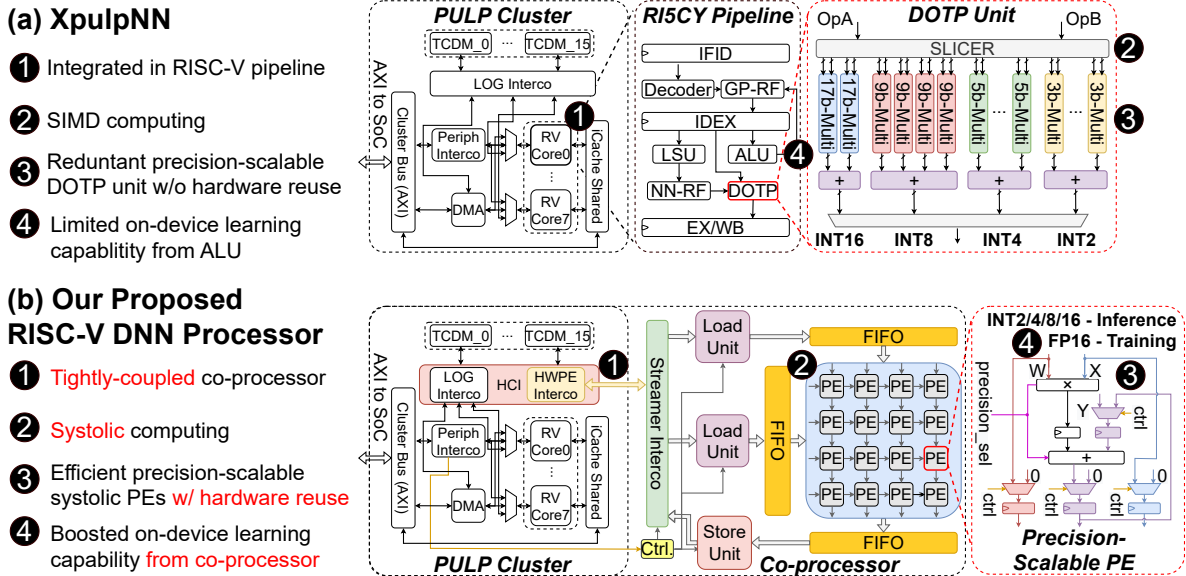


Fig. 1. Comparison between the architecture of (a) XpulpNN [20] and (b) our proposed DNN processor.

multiplier of PEs to support FP16 operations, a maximum $16.5\times$ on-device learning throughput improvement is achieved, while LUT and DSP utilization are increased by 4.7% and 64.3%, respectively, compared to XpulpNN.

II. RELATED WORKS

Extreme edge processors are dominated by ARM or RISC-V instruction-driven microcontrollers. These devices face severe constraints on energy, memory, and computing, while confronting a substantial demand for deploying DNNs to realize intelligent applications. To tackle these challenges, prior works [1]–[5] propose several dedicated DNN accelerators, but they sacrifice the general support for instruction-driven MCUs in extreme edge platforms across various IoT nodes. Moreover, [7]–[10] only support a single data type, limiting their effectiveness in deploying various quantized DNNs with precision ranging from INT2 to INT16 [1], [2], [4], [5].

In contrast, enhancing throughput of RISC-V processors for quantized DNNs [6], [11], [14]–[16], [20] shows greater potential compared to exploiting dedicated DNN accelerators. It maintains general support of RISC-V instructions, decouples software development and hardware implementation, and achieves significant performance in deploying DNNs. Among them, FlexACC [6] and RedMule [11] enable only 8-bit or higher precision for DNN inference, which can hardly leverage the computational reduction potential of lower-bit quantized DNNs. The other RISC-V processors [14]–[16], [20] achieves significant speedup by supporting lower-bit DNN inference. In addition, on-device learning at the extreme edge has gained attention for improving the accuracy of quantized DNNs while safeguarding data privacy. Nevertheless, both BARVINN [15] and [16] remove FP support, rendering them incapable of on-device learning. XpulpNN [20] and Dustin [14] have weak on-device learning capability from the arithmetic logic unit (ALU) supporting FP operations in the RISC-V pipelines.

Compared with the above prior arts, our proposed RISC-V DNN processor not only efficiently supports precision-scalable quantized DNN inference varying from INT2 to INT16 but also significantly enhances on-device learning capability.

III. THE PROPOSED RISC-V DNN PROCESSOR

A. Features of Our DNN Processor

PULP [21] is an open-source RISC-V computing platform with a primary focus on achieving high energy efficiency. The RISC-V cores of a PULP cluster can be extended, and the cluster is equipped with a heterogeneous cluster interconnect (HCI) for memory access, dataflow control, and controlling customized co-processors. Fig. 1 (a) presents XpulpNN [20], the state-of-the-art RISC-V processor based on the PULP platform, which enables precision-scalable DNN inference with limited on-device learning capability. By contrast, as shown in Fig. 1 (b), we propose a precision-scalable DNN processor based on the PULP platform, which significantly promotes multi-precision computing and on-device learning capability on DNNs over XpulpNN. Compared to XpulpNN, our proposed processor stands out due to the following features:

1 Resource-efficient tightly-coupled co-processor. The proposed co-processor is connected with the PULP cluster through the HWPE interface, which is more resource-efficient than XpulpNN. The proposed co-processor achieves higher throughput by incorporating extra embedded PEs, while XpulpNN requires adding more RISC-V cores to attain improved throughput, resulting in additional associated overhead.

2 High-throughput systolic computing. To perform matrix multiplication (matmul) operations dominated in DNNs efficiently, a high-throughput SA is proposed. It requires only one instruction to initiate computation, reducing the number of compute instructions and cycles, thus increasing throughput. The throughput can be further improved by implementing

more PEs in the SA. Compared to XpulpNN which requires more instructions for the same SIMD matmul and contains only four INT8 operating units per RISC-V core, the SA achieves more efficient computations and higher throughput.

③ **Resource-efficient precision-scalable PEs.** The constraints posed by limited hardware resources at the extreme edge make it important to improve hardware resource utilization. To address this, we present precision-scalable PEs that minimize resource redundancy through multiple carefully designed hardware reuse techniques. Our PEs achieve higher resource utilization compared to XpulpNN’s dotp units that have no reuse on multipliers supporting various precision.

④ **Boosted on-device learning capability.** To better support on-device learning at extreme-edge, floating-point computation throughput needs to be increased. Therefore, our processor natively supports FP16-based computation in the PEs, rather than performing floating-point operations using the FPU embedded in the ALU, as XpulpNN does. The improved floating-point computation capability enables our processor to achieve higher throughput as well as on-device learning efficiency.

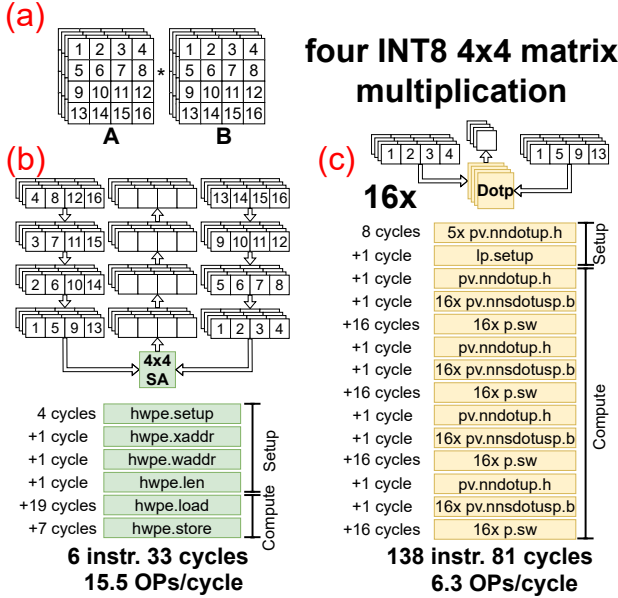


Fig. 2. The instruction and computation flow of our processor and XpulpNN to perform an INT8 matrix multiplication operator. (a) shows the 4×4 matmul operator; (b) and (c) show the computational and instruction flows of our processor’s SA and XpulpNN’s dotp units, respectively.

B. Customized RISC-V Instruction-Driven Mapping

Our processor demonstrates superior computational efficiency over XpulpNN with same multiply-accumulate (MAC) units when executing the same matmul. As shown in Fig. 2, both XpulpNN and our processor need setup and compute instructions to initialize the computation and subsequently execute operators, respectively. However, our processor excels benefiting from more efficient initialization and execution. For instance, it only takes 4 instructions (7 cycles) to setup, and another 2 instructions (26 cycles) to compute when employed four 4×4 INT8-based operators. Our processor uses merely 4% instructions and 41% cycles required by XpulpNN, which needs 6 instructions (9 cycles) and 132 instructions (72 cycles)

to setup and compute, respectively. The significant reduction in number of instructions and cycles contributes to a 2.5× throughput improvement for our processor, thereby achieving higher computational efficiency than XpulpNN.

Specifically, a more efficient setup is first introduced to improve the computational efficiency. XpulpNN needs to initialize each loop when setting up the computation demonstrated in Fig. 2 (c), whereas our processor only needs hwpe.setup to perform the overall initialization (including startup and precision configuration), hwpe.xaddr and hwpe.waddr to read the first addresses of input matrix A and B, respectively, and hwpe.len to determine the data length, as shown in Fig. 2 (b).

In addition, a more efficient computation is also implemented. For XpulpNN, it needs multiple load and store instructions to compute all the operators, since a single dotp unit can only perform the dot-product of two vectors of length 4 per instruction, as shown in Fig. 2 (c). By contrast, our processor only needs one instruction to load all the data into the SA to compute (hwpe.load) and one instruction to store all the results (hwpe.store), as shown in Fig. 2 (b).

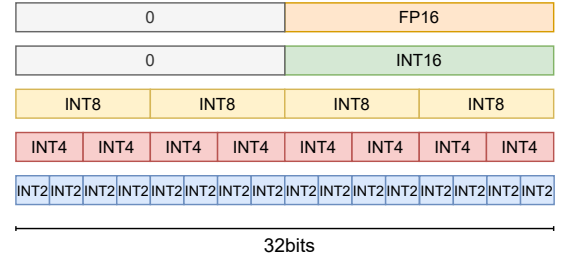


Fig. 3. Data arrangement method of different precision.

C. Precision-Scalable Processing Element

Fig. 1 shows a precision-scalable PE utilized for highly-parallel precision-scalable MAC operations. Each PE comprises precision-scalable adder and multiplier, as well as registers and multiplexers (MUXs) for data flow direction control. The mode of the SA determines whether the 64-bit output data Y is temporarily stored inside the PE or shifted out. During computation, 32-bit input data X and W are sequentially shifted in. Controlled by a precision selection signal, a PE can efficiently compute a single FP16 MAC, a single INT16 MAC, four-parallel INT8 MACs, eight-parallel INT4 MACs, or sixteen-parallel INT2 MACs on-the-fly.

To accommodate precision-scalable PEs, a specific data arrangement method is devised to reduce overall computation time by ensuring the co-processor efficiently processes data with different precision. Data with varying quantization length are organized in a manner depicted in Fig. 3. Specifically, every four, eight, and sixteen data are grouped as a single 32-bit data in 8-bit, 4-bit, and 2-bit precision, respectively. For 16-bit INT16 and FP16 data, each of them is padded with an additional 16 bits of 0, transforming it into 32-bit data.

Precision-Scalable Multiplier. To efficiently support multi-precision INT multiplication for inference and FP16 multiplication for on-device learning, we propose the precision-scalable multiplier shown in Fig. 4, which contains of one

16-bit multiplier and four 8-bit precision-scalable multiplier trees. The FP16-based mantissa multiplier reuses the hardware resources of the INT16 multiplier, while the multiplier trees are used for parallel INT8, INT4 or INT2 multiplications. According to the precision selection signal, the inputs are sliced into different bit-widths and fed into different multipliers, and then the corresponding spliced data is selected as the outputs. With this precision-scalable multiplier, the hardware resources of one additional 16-bit multiplier are saved.

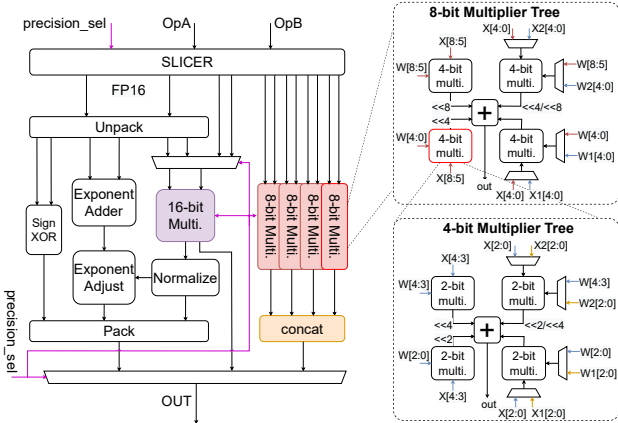


Fig. 4. Architecture of the precision-scalable multiplier with highly-reused 16-bit mantissa multiplier and 8-bit multiplier trees. Only half of the 4-bit multiplier trees and 2-bit multipliers of one 8-bit multiplier tree are reused to ensure the output bit-width remains the same at different precision levels.

8-bit Multiplier Tree. The 8-bit precision-scalable multiplier tree shown in Fig. 4 further supports efficient computation of INT8, INT4, and INT2 multiplications. Each 8-bit tree consists of four 4-bit precision-scalable multiplier trees and one adder, and is capable of performing single 8-bit multiplication through shift-and-add of partial products. Different from [23], a single 8-bit tree also perform two 4-bit multiplications using two parallel 4-bit multiplier trees. Similarly, the 4-bit tree performs single INT4 multiplication or two INT2 multiplication in parallel. This architecture saves hardware resources that would have been allocated to eight 4-bit multipliers and sixteen 2-bit multipliers, resulting in reduced LUT overhead for the PE compared to the unused dotp unit of XpulpNN.

Precision-Scalable Adder. In addition, we present the precision-scalable adder shown in Fig. 5 for implementing INT16, INT8, INT4, INT2 and FP16 addition to fully support precision-scalable computation and on-device learning. It consists of one FP16 floating point adder, one 32-bit adder, four 16-bit adders, eight 8-bit adders and sixteen 4-bit adders. Unlike precision-scalable multiplier, the adder is not reused with varying precision, for that the additional overhead caused by the increased MUXs is found to be close to the hardware resources it aims to reduce.

D. Balancing LUT and DSP Mapping

For the implementation of the proposed processor architecture with FPGA devices, the computational logic is mapped to available resources including DSPs and LUTs. However,

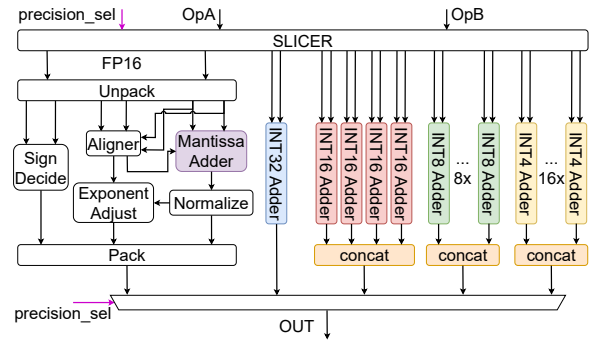


Fig. 5. Architecture of the precision-scalable adder.

automatic resource mapping often leads to inefficiencies, such as high LUT overhead or low DSP utilization in XpulpNN. To address this, we adopt a mapping approach to ensure high resource utilization for both DSPs and LUTs. In particular, the 16-bit mantissa multiplier illustrated in Fig. 4 is mapped to DSPs, while four 8-bit precision-scalable multiplier trees are mapped to LUTs. Moreover, the INT adders shown in Fig. 5 are mapped to DSPs, while the FP16 adder is mapped to LUTs. This balanced mapping approach ensures efficient utilization of FPGA resources, including both DSPs and LUTs, in our design. By adopting this method, we can reduce the consumption of LUTs compared to approaches that exclusively map to LUTs, as well as relieve the over-consumption of DSPs compared to methods that primarily rely on DSP mapping.

IV. EXPERIMENTAL RESULTS

A. Experimental Setup

We synthesize our precision-scalable RISC-V DNN processor using Vivado 2018.3 and implement it on two FPGA boards: ZCU102 and PYNQ-Z2, with a clock frequency of 200MHz and 100MHz, respectively. The size of SAs in our processors deployed on ZCU102 and PYNQ-Z2 are 12×12 and 4×4 , respectively. The widely-used DNN models are selected for evaluation of DNN deployment, including MobileNetv2, VGG-16, ResNet-18, ResNet-50, and ViT/B-16. We follow the experimental methods in BARVINN [15] and evaluate the throughput by operators of convolutional layers and fully connected layers. Power consumption is estimated using the Vivado Power Analysis tool. For a fair comparison against our processor, ARM-Cortex A7 and i5-10505 are selected as CPU baselines, and Jetson Nano is selected as a GPU baseline, which is a commercial product for DNN deployment at the extreme edge. Additionally, we implement an 8-core XpulpNN [20] on a ZCU102 board running at 200MHz as an FPGA baseline. The other FPGA-based state-of-the-arts [7]–[10], [13], [15] are also selected as our baselines.

B. FPGA Resource Utilization Analysis

Reuse of Hardware Resources. The extreme-edge platform uses FPGAs with very few on-chip resources, pressing the need to reuse hardware resources for precision-scalable inference and on-device learning. Fig. 6 illustrates the comparison of consumed FPGA resources on ZCU102 between

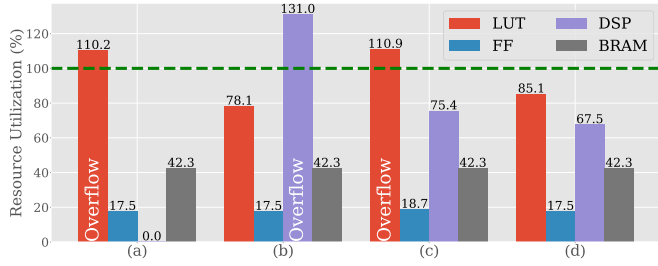


Fig. 6. Utilization using different resource mapping methods on ZCU102: (a) mapping to LUTs only with reused multipliers; (b) mapping to DSPs whenever possible with reused multipliers; (c) balanced mapping to LUTs and DSPs without reused multipliers; (d) balanced mapping to LUTs and DSPs with reused multipliers.

the different mapping methods in III-C & III-D. Utilizing the balanced method with reused multipliers as shown in Fig. 6 (d) achieves 85.1% LUT utilization and 67.5% DSP utilization. It consumes 25.1% fewer LUTs than mapping to LUTs only with reused multipliers in (a), 63.9% fewer DSPs than mapping to DSPs whenever possible with reused multipliers in (b), 25.8% fewer LUTs and 7.9% fewer DSPs than mapping to LUTs and DSPs with the balanced method with unreused multipliers in (c). Furthermore, (d) is the only approach that does not cause resource overflow. These results demonstrate the effectiveness of our proposed methods in III-C & III-D, which significantly improve LUT and DSP utilization while reducing unnecessary hardware resource overhead.

Overhead for On-Device Learning Support. The extreme-edge platform introduces additional hardware resource overhead to support floating-point computation for on-device learning. Hence, we evaluate the hardware resource consumption of our processor with and without FP16 computation capability, and compare it with XpulpNN [20] and Angel Eye [10], where XpulpNN supports precision-scalable together with floating-point computation, and Angel Eye has decent throughput at INT16 precision despite lacking the precision-scalable capability. As shown in Fig. 7, our processor has 28.1% LUT overhead and 15.9% DSP overhead when adding FP16 support, while FF and BRAM have essentially no additional overhead. However, the processor achieves 57.6 GOPs of FP16 theoretical throughput. Compared to XpulpNN [20] and Angel Eye [10], our processor increases DSP utilization by 64.3% and 36.5%, and LUT utilization by 4.7% and 18.5%, respectively. Furthermore, by supporting multi-precision and on-device learning, our processor achieves significant theoretical throughput improvement compared to XpulpNN (16.5 \times at FP16, 8.2 \times at INT8, INT4, and INT2) and Angel Eye (1.2 \times at INT8, 2.5 \times at INT4 and 4.9 \times at INT2).

C. Throughput and Energy Efficiency Comparison

Extreme edge platforms have stringent requirements for low DNN inference latency and are also very sensitive to power consumption. Hence, throughput and energy efficiency are critical metrics for efficient DNN inference. We employ our processor to deploy diverse DNN models of varying precision and make a comparison of throughput and energy efficiency between our processor and baselines. The experimental re-

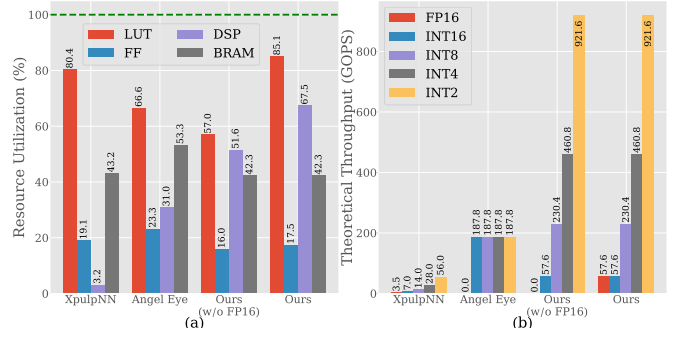


Fig. 7. Hardware resources and theoretical throughput of different works on ZCU102. Compared to XpulpNN, DSP and LUT utilization are increased by 64.3% and 4.7%, respectively. Furthermore, the theoretical throughput of our processor is increased by 16.5 \times (FP16) and 8.2 \times (INT8, INT4, and INT2).

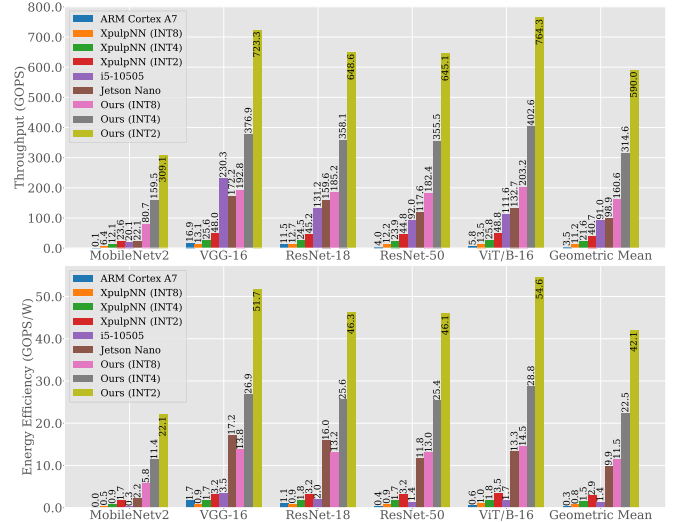


Fig. 8. Comparison of throughput and energy efficiency under various DNN models. Our processor achieves 1.6 \times and 14.3 \times average INT8 throughput improvement and 1.2 \times and 14.4 \times average INT8 energy efficiency improvement over Jetson Nano and XpulpNN, respectively.

sults in Fig. 8 shows our processor achieves considerable throughput and energy efficiency on average (160.6 GOPs and 11.5 GOPs/W at INT8, 314.6 GOPs and 22.5 GOPs/W at INT4, 590.0 GOPs and 42.1 GOPs/W at INT2). In addition, 1.6 \times and 14.3 \times INT8 throughput improvement over Jetson Nano and XpulpNN, respectively, is achieved on average by our processor. Furthermore, our processor demonstrates substantial advancements in energy efficiency, with an average improvement of 14.6 \times and 14.5 \times over XpulpNN for INT4 and INT2 precision, respectively. Compared to Jetson Nano, our processor achieves 1.1~3.9 \times and 1.1~4.1 \times energy efficiency improvements on ResNet-50 and ViT/B-16 at various precision, respectively, and it achieves 2.6~10.0 \times higher energy efficiency improvements when running a lower computational density network, i.e., MobileNetv2, at various precision.

D. Comparison to CPU, GPU, and FPGA-based Prior Arts

To evaluate the improvement of our processor on various metrics, we make a comprehensive comparison with CPUs, GPU, and FPGA-based prior works, as detailed in Table I. Compared to CPUs such as i5-10505 and Arm Cortex A7,

TABLE I
COMPARISON TO RELATED WORKS

Work	Platform	kLUTs	DSPs	Frequency (MHz)	Model	Throughput (GOPS)				Energy Efficiency (GOPS/W)				On-Device Learning FP Support
						INT16	INT8	INT4	INT2	INT16	INT8	INT4	INT2	
Baseline 1	Arm Cortex A7	-	-	1430	ResNet-50	4.0	N/A	×	×	0.4	N/A	×	×	✓
Baseline 2	i5-10505	-	-	3200	ResNet-50	92.0	N/A	×	×	1.4	N/A	×	×	✓
Baseline 3	Jetson Nano	-	-	640	ResNet-50	N/A	117.6	×	×	N/A	11.8	×	×	✓
Going Deeper [8]	XC7Z045	218.6	N/A	150	VGG-16	137.0	×	×	×	N/A	×	×	×	×
Angel Eye [10]	XC7Z045	182.6	780	150	VGG-16	187.8	×	×	×	14.2	×	×	×	×
ThroughputOpt [7]	Stratix V	153	246	120	VGG-16	×	117.8	×	×	×	N/A	×	×	×
Mix and Match [9]	XC7Z045	145.1	900	100	ResNet-18	×	×	359.2	×	×	×	N/A	×	×
FILM-QNN [13]	ZCU102	174.5	2.1k	150	ResNet-50	×	N/A	387.8	×	×	N/A	28.9	×	×
BARVINN [15]	Alveo U250	201.1	512	250	ResNet-50	N/A	N/A	N/A	380.4	N/A	N/A	N/A	17.7	×
XpulpNN [20]	ZCU102	220.4	80	200	ResNet-50	6.0	12.2	23.9	44.8	0.4	0.9	1.7	3.2	✓
Ours	PYNQ-Z2	32.9	190	100	ResNet-50	2.8	11.8	24.3	46.5	0.7	3.0	6.1	11.6	✓
Ours	ZCU102	233.3	1.7k	200	ResNet-50	47.0	182.4	355.5	645.1	3.4	13.0	25.4	46.1	✓

our processor achieves noteworthy energy efficiency enhancements of $2.4\times$ and $8.5\times$, respectively, at INT16 precision on ZCU102. Additionally, it outperforms the energy-efficient GPU, Jetson Nano, with a throughput improvement of $1.6\times$ and an energy efficiency improvement of $1.1\times$. When compared to FPGA-based XpulpNN [20] that supports precision-scalable inference and on-device learning, significant improvements in throughput by $7.8\sim 15.0\times$ and energy efficiency by $8.5\sim 14.4\times$ have been achieved by our processor on ZCU102 at different precision. Our processor uniquely offers both precision scalability ranging from INT16 to INT2 and on-device learning capability with FP16 support, setting it apart from prior FPGA-based arts [7]–[10], [13], [15]. Furthermore, our processor on ZCU102 improves throughput by $1.6\sim 1.7\times$ when compared to these works. Finally, our processor can accommodate various FPGA platforms with different amount of hardware resources. When deployed on PYNQ-Z2, it achieves comparable throughput and $1.8\sim 3.6\times$ energy efficiency gains compared to XpulpNN at INT8, INT4, and INT2 precision.

V. CONCLUSION

In this paper, we propose a high-throughput, energy-efficient and precision-scalable RISC-V DNN processor with on-device learning capability at the extreme edge to address the growing needs for DNN deployment. Furthermore, precision-scalable processing elements with boosted on-device learning throughput are proposed, and the hardware resources are fully leveraged by several methods. Our proposed processor increases LUT and DSP utilization by 4.7% and 64.3%, respectively, and achieves up to $14.6\times$ improvement of inference throughput and energy efficiency on average compared to the existing XpulpNN solutions when computing various quantized DNNs. It also achieves up to $16.5\times$ on-device learning throughput improvement compared to XpulpNN.

ACKNOWLEDGMENT

This work was supported in part by the National Key R&D Program of China under Grant 2022YFB4400604, in part by the National Natural Science Foundation of China under Grant 62174084, and in part by the Postgraduate Research & Practice Innovation Program of Jiangsu Province under Grant SJCX23_0016.

REFERENCES

- [1] J. Wu *et al.*, “Quantized convolutional neural networks for mobile devices,” in *CVPR*, 2016.
- [2] Z. Liu *et al.*, “Post-training quantization for Vision Transformer,” *NeurIPS*, 2021.
- [3] R. Ding *et al.*, “Quantized deep neural networks for energy efficient hardware-based inference,” in *ASP-DAC*, 2018.
- [4] J. Tian *et al.*, “BEBERT: Efficient and robust binary ensemble BERT,” in *ICASSP*, 2023.
- [5] A. Zhou *et al.*, “Explicit loss-error-aware quantization for low-bit deep neural networks,” in *CVPR*, 2018.
- [6] E.-Y. Yang *et al.*, “FlexACC: A programmable accelerator with application-specific ISA for flexible deep neural network inference,” in *ASAP*, 2021.
- [7] N. Suda *et al.*, “Throughput-optimized OpenCL-based FPGA accelerator for large-scale convolutional neural networks,” in *FPGA*, 2016.
- [8] J. Qiu *et al.*, “Going deeper with embedded FPGA platform for convolutional neural network,” in *FPGA*, 2016.
- [9] S.-E. Chang *et al.*, “Mix and Match: A novel fpga-centric deep neural network quantization framework,” in *HPCA*, 2021.
- [10] K. Guo *et al.*, “Angel-Eye: A complete design flow for mapping CNN onto embedded FPGA,” *TCAD*, 2017.
- [11] Y. Tortorella *et al.*, “RedMulE: A compact FP16 matrix-multiplication accelerator for adaptive deep learning on RISC-V-based ultra-low-power SoCs,” in *DATe*, 2022.
- [12] H. Cai *et al.*, “TinyTL: Reduce memory, not parameters for efficient on-device learning,” *NeurIPS*, 2020.
- [13] M. Sun *et al.*, “FILM-QNN: Efficient fpga acceleration of deep neural networks with intra-layer, mixed-precision quantization,” in *FPGA*, 2022.
- [14] G. Ottavi *et al.*, “Dustin: A 16-cores parallel ultra-low-power cluster with 2b-to-32b fully flexible bit-precision and vector Lockstep execution mode,” *TCAS-I*, 2023.
- [15] M. Askarihemmat *et al.*, “BARVINN: Arbitrary precision DNN accelerator controlled by a RISC-V CPU,” in *ASP-DAC*, 2023.
- [16] Z. He *et al.*, “Agile hardware and software co-design for RISC-V-based multi-precision deep learning microprocessor,” in *ASP-DAC*, 2023.
- [17] X. Wu *et al.*, “A flexible and efficient FPGA accelerator for various large-scale and lightweight CNNs,” *TCAS-I*, 2021.
- [18] C. Fang *et al.*, “Accelerating 3D convolutional neural networks using 3D fast Fourier transform,” in *ISCAS*, 2021.
- [19] H. Wang *et al.*, “A low-latency sparse-winograd accelerator for convolutional neural networks,” in *ICASSP*, 2019.
- [20] A. Garofalo *et al.*, “XpulpNN: Enabling energy efficient and flexible inference of quantized neural networks on risc-v based iot end nodes,” *TETC*, 2021.
- [21] F. Conti *et al.*, “PULP: A ultra-low power parallel accelerator for energy-efficient and flexible embedded vision,” *JSPS*, 2016.
- [22] P. Micikevicius *et al.*, “Mixed precision training,” *ICLR*, 2018.
- [23] H. Sharma *et al.*, “Bit Fusion: Bit-level dynamically composable architecture for accelerating deep neural network,” in *ISCA*, 2018.